Subwavelength Discrete Solitons in Nonlinear Metamaterials

Yongmin Liu, Guy Bartal, Dentcho A. Genov, and Xiang Zhang*

NSF Nanoscale Science and Engineering Center (NSEC), 5130 Etcheverry Hall, University of California, Berkeley, California 94720-1740, USA

(Received 21 March 2007; published 12 October 2007)

We present the first study of subwavelength discrete solitons in nonlinear metamaterials: nanoscaled periodic structures consisting of metal and nonlinear dielectric slabs. The solitons supported by such media result from a balance between tunneling of surface plasmon modes and nonlinear self-trapping. The dynamics in such systems, arising from the threefold interplay between periodicity, nonlinearity, and surface plasmon polaritons, is substantially different from that in conventional nonlinear dielectric waveguide arrays. We expect these phenomena to inspire fundamental studies as well as potential applications of nonlinear metamaterials, particularly in subwavelength nonlinear optics.

DOI: 10.1103/PhysRevLett.99.153901 PACS numbers: 42.65.Tg, 73.20.Mf, 78.67.Pt

Metamaterials have recently attracted widespread interest due to their intriguing properties not found in naturally occurring materials, and their potential for new applications such as negative refraction, reversed Doppler effect, and Cerenkov radiation [1,2], as well as electromagnetic (EM) cloaking of arbitrary shaped objects [3]. There has been a growing interest in nonlinear metamaterials as they exhibit new types of nonlinear phenomena such as second-harmonic generation from split-ring resonators [4], discrete breathers in split-ring arrays [5], and controllable transition between left-handed and right-handed material properties [6]. Metamaterials also provide an excellent means to pursue subwavelength optics, which has great impact on imaging, lithography, sensing, and data storage. The strong modal confinement of surface plasmon polaritons (SPPs) in metal-dielectric composites [7], was utilized to demonstrate extraordinary transmission through subwavelength hole arrays [8] and subdiffraction-limited imaging with superlens [9].

An important subset of metamaterials is subwavelength metal-dielectric multilayers (MDMLs): periodic structures consisting of nanoscaled metallic and dielectric slabs [10]. In these structures, SPPs can tunnel between adjacent layers giving rise to Bloch-like modes carrying the signature of the SPPs [11]. MDMLs have also been studied in the nonlinear regime, where the relatively high nonlinear coefficient of copper was utilized [12,13]. In what follows, we show that a MDML with nonlinear (Kerr-type) dielectric can exhibit self-focusing of light, and form subwavelength discrete solitons characterized by intriguing features that have not been reported so far.

Discrete (or ''lattice'') solitons have been observed in many areas of science, such as biology [14], solid state physics [15], and Bose-Einstein condensates (BEC) [16]. In optics, solitons in nonlinear lattices have been proposed [17] and observed in dielectric waveguide arrays (DWGAs) under self-focusing [18,19] and self-defocusing [20,21] nonlinearities. In these settings, the nonlinearity can balance the light tunneling between neighboring waveguides, resulting in self-localization and stationary propagation. Subsequent investigations have analyzed lattice solitons that originate from higher bands [22,23]. In all previous work, the soliton dimension and the periodicity of the system are much larger than the excitation wavelength.

Here, we present the first study of subwavelength discrete solitons in nonlinear MDMLs, at visible and near-infrared frequencies. These solitons manifest unique features arising from the threefold interplay between periodicity, nonlinearity, and SPPs tunneling, and display anomalous behaviors comparing to solitons in uniform dielectric media and conventional DWGAs.

We start by calculating the eigenmodes of a linear MDML, schematically shown in Fig. 1(a). In contrast to [17–24], the assumptions of the slowly varying amplitude and small variation in the dielectric function are no longer valid for subwavelength structures as discussed here. We derive the governing eigenproblem directly from Maxwell's equations

$$\nabla \times \vec{H} = \frac{1}{c}\frac{\partial(\varepsilon \vec{E})}{\partial t}, \qquad \nabla \times \vec{E} = -\frac{1}{c}\frac{\partial(\mu \vec{H})}{\partial t} \tag{1}$$

where c is the speed of light in vacuum, $\vec{E}$ and $\vec{H}$ are the electric and magnetic fields, respectively, $\varepsilon(x, z)$ is the spatially varying dielectric permittivity, and the magnetic permeability μ is set to be 1. We solve Eq. (1) for time-harmonic propagation along the z axis, taking into account the transverse magnetic (TM) nature of the SPPs waves [7] [i.e., $\vec{H} = H_y\hat{y}$ and $\vec{E} = E_x\hat{x} + E_z\hat{z}$, see the coordinates in Fig. 1(a)]. By properly rearranging Eq. (1), and introducing a ''Hamiltonian'' operator $\hat{H}(x) = \frac{\partial}{\partial x}(\frac{1}{\varepsilon}\frac{\partial}{\partial x}) + k_0^2$, it is straightforward to obtain an explicit matrix form

$$\frac{\partial}{\partial z}\begin{pmatrix} H_y \\ E_x \end{pmatrix} = -\frac{i}{k_0}\begin{pmatrix} 0 & \varepsilon k_0^2 \\ \hat{H} & 0 \end{pmatrix}\begin{pmatrix} H_y \\ E_x \end{pmatrix} \tag{2}$$

where $k_0 = 2\pi/\lambda_0$ (λ_0 is the wavelength in vacuum).

The EM eigenmodes of such a system maintain their envelopes during propagation, that is,

$$H_y(x, z) = \tilde{H}_y(x)e^{-i\beta z} \qquad E_x(x, z) = \tilde{E}_x(x)e^{-i\beta z} \tag{3}$$

 © 2007 The American Physical Society

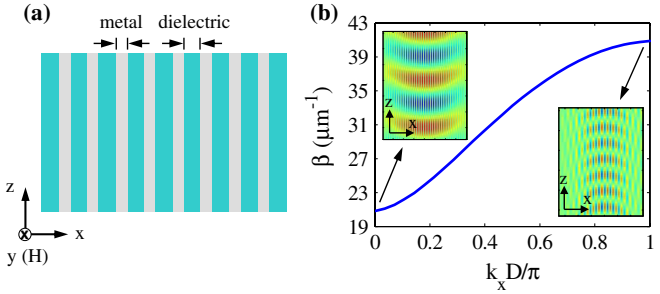

FIG. 1 (color online). (a) Schematic of MDMLs. (b) Diffraction-relation diagram (propagation constant vs transverse momentum). The insets show the transverse electric field of a diffracting narrow beam originating from the $k_x = 0$ and $k_x = \pi/D$ points in the momentum space.

where β indicates the propagation constant. Substituting Eq. (3) into Eq. (2) we obtain the eigenvalue problem

$$\hat{M}(x)\vec{\Psi}(x) = \beta\vec{\Psi}(x), \qquad \hat{M}(x) = \frac{1}{k_0}\begin{pmatrix} 0 & \varepsilon k_0^2 \\ \hat{H}(x) & 0 \end{pmatrix} \quad (4)$$

where $\vec{\Psi} = (\tilde{H}_y, \tilde{E}_x)^T$.

The eigenproblem in Eq. (4) is calculated numerically by considering the boundary conditions for the EM fields at the metal-dielectric interfaces. The solutions of Eq. (4) form a set (or a band) of eigenvalues representing the linear propagation constants supported by the system [11]. In what follows, we choose the dielectric slab width $t_d = 26$ nm, and metal slab width $t_m = 16$ nm. The dielectric linear refractive index is $n = \sqrt{\varepsilon_d} = 1.5$, and the metal relative permittivity at $\lambda_0 = 632.8$ nm is taken to be $\varepsilon_m = -17$ (the effect of metal loss will be discussed later) [25]. The variation of β with the transverse momentum k_x shown in Fig. 1(b) presents a trend opposite to the one for conventional DWGAs. Namely, $\beta(k_x = 0)$ is smaller than $\beta(k_x = \pi/D)$. Interestingly, the modal profiles of tangential fields are identical to those of the second-band modes of a paraxial DWGA [23], and correspond to "negative" coupling between neighboring waveguides. As a result, the curvature of the band (i.e., the 2nd derivative) is positive at $k_x = 0$, and negative at $k_x = \pi/D$, indicating that the diffraction of a localized wave packet is anomalous at $k_x = 0$ and normal at $k_x = \pi/D$, in a sharp contrast to what is observed in DWGAs [24]. This phenomenon is presented by the insets in Fig. 1(b), where a narrow wave packet at $k_x = 0$ ($k_x = \pi/D$) is shown to acquire a concave (convex) phase front as it propagates through the media and diffracts.

Such diffraction, resulting from SPPs tunneling between neighboring layers, can be arrested when the refractive index of the dielectric layers is intensity dependent. For example, the permittivity of Kerr optical materials varies linearly with the intensity, namely, $\varepsilon(|\vec{E}|^2) = \varepsilon_r + 2\alpha\sqrt{\varepsilon_r}n_2|\vec{E}|^2$, where $\vec{E}$ is the local electric field, ε_r the linear relative permittivity, n_2 is the Kerr coefficient, and $\alpha = +1$ ($\alpha = -1$) correspond to self-focusing (self-defocusing) nonlinearity. As self-focusing (defocusing) nonlinearity can balance normal (anomalous) diffraction [17–21], solitons originating at $k_x = \pi/D$ ($k_x = 0$) will form under a self-focusing (defocusing) nonlinearity.

We utilize the self-consistency method [23] to solve Eq. (4) in the nonlinear case. The solution provides the transverse magnetic ($\tilde{H}_y$) and electric ($\tilde{E}_x$) fields of the nonlinear eigenmodes. Then, the longitudinal electric field ($\tilde{E}_z$) can be directly derived from Maxwell's equations, that is, $\tilde{E}_z = -i(k_0\varepsilon)^{-1}\partial\tilde{H}_y/\partial x$.

The electric fields of the nonlinear localized modes are given in Fig. 2(a) for the mode originating at the $k_x = 0$ point (under self-defocusing nonlinearity), and in Fig. 2(c) for the mode originating in $k_x = \pi/D$ (under self-focusing nonlinearity). The intensities of these two localized modes are presented in Figs. 2(b) and 2(d), respectively. For maximum nonlinear index change of $\Delta n_{\max} = 0.04$ [26], the mode at $k_x = \pi/D$ displays a full width at half maximum (FWHM) of 190 nm, smaller than the diffraction limit in the dielectric host ($1.22\lambda_0/2n \approx 250$ nm). On the other hand, the mode at $k_x = 0$ has a much broader FWHM for the same magnitude of nonlinear index change (but with an opposite sign), due to the different magnitudes of the band curvature at $k_x = 0$ and at $k_x = \pi/D$. The larger band curvature at $k_x = 0$ results in a beam diffraction that is stronger than that around the $k_x = \pi/D$ point. Since the soliton is a result of the balance between diffraction and nonlinearity, the same magnitude of nonlinearity will result in a larger mode size at $k_x = 0$. This is in sharp contrast to the discrete systems discussed in [17–21], where the band structure is approximated by $\cos(k_x D)$ ("tight binding model").

In order to study the actual propagation of a soliton in the MDML, we use a modified form of the "split-step Fourier" beam propagation method (BPM) [27]. The propagation operator $\hat{M}$ is taken to be the sum of two operators, that is, $\hat{M}(z) = \hat{M}_L + \hat{M}_{\mathrm{NL}}(z)$ with $\hat{M}_L$ representing the linear propagation in the MDMLs [28], while $\hat{M}_{\mathrm{NL}}$ is the contribution of the nonlinear index change. The fields at the point $z + \Delta z$ along the propagation direction can be obtained from the fields at z, namely $\vec{\Psi}(z + \Delta z) = \exp(\hat{M}_{\mathrm{NL}}\Delta z)\exp(\hat{M}_L\Delta z)\vec{\Psi}(z)$. This way, we simulate the propagation of an initial mode profile $\vec{\Psi}(0)$ calculated by the self-consistency method. In what follows, we focus on the propagation of the localized mode from $k_x = \pi/D$, as it features subwavelength characteristics for the parameters given above.

Figures 2(e) and 2(f) present the propagation simulations over 4 μm in linear and nonlinear MDMLs, respectively. At low intensities, SPPs tunnel between neighboring slabs, resulting in linear diffraction of the initial wave packet [Fig. 2(e)]. However, when the proper intensity (calculated by the self-consistency method) is applied, the wave packet maintains its original shape during propagation [Fig. 2(f)]. Comparing Figs. 2(e) and 2(f) clearly demonstrates the self-focusing effect and the formation of the lattice solitons under proper nonlinearity.

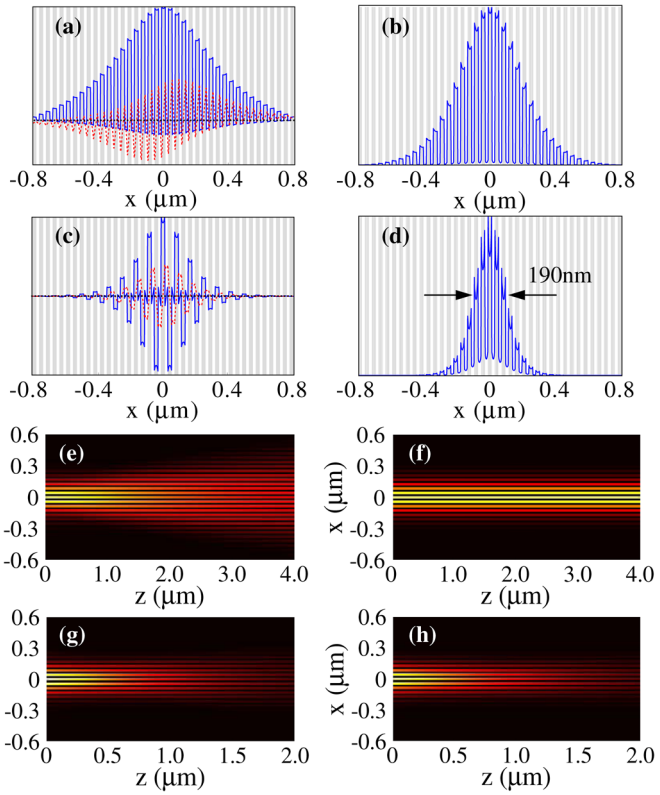

FIG. 2 (color online). Nonlinear localized EM modes in MDMLs with period of 42 nm at an incident wavelength of 632.8 nm. (a),(c) Transverse ($\tilde{E}_x$, solid line) and longitudinal ($\tilde{E}_z$, dashed line) electric field distributions of the solitons arising from the points in momentum space, $k_x = 0$ and $k_x = \pi/D$, respectively. The horizontal dotted line indicates the zero field. The white and shaded regions represent the metal and dielectric slabs, respectively. (b),(d) Intensity distribution of the same modes. (e) Linear and (f) nonlinear propagation of the $k_x = \pi/D$ mode over 4 μm distance in lossless MDMLs. (g) Linear and (h) nonlinear propagation of the same mode along 2 μm in a MDML when the silver's loss is taken into account.

The soliton propagation along a MDML can be dramatically affected by the mode's power dissipation in the metal, as shown in Figs. 2(g) and 2(h). Although Ohmic loss is an intrinsic property of the metal and depends solely on the incident frequency, the dissipation of a given mode depends on the system's geometry and varies between the system's eigenmodes according to the modal distribution; i.e., a mode with a large portion of its electric field residing in the metal will experience high loss. Figures 2(c) and 2(d) depict the substantial electric field inside the metal at $k_x = \pi/D$, hence, one can expect a higher mode loss. The dissipation coefficient can be directly obtained from the imaginary part of the propagation constant β, calculated from Eq. (4) for a complex metal permittivity ($\varepsilon_m = -17 + 0.69i$ for silver at 632.8 nm [25]). The dissipation coefficient is $2\,\mathrm{Im}(\beta_0) = 658\ \mathrm{cm}^{-1}$ for the $k_x = 0$ mode, and $2\,\mathrm{Im}(\beta_{\pi/D}) = 7800\ \mathrm{cm}^{-1}$ for the $k_x = \pi/D$ mode, which corresponds to the decay length of 15.2 and 1.3 μm, respectively. The decay length of the $k_x = \pi/D$ mode is shorter than its diffraction length (the distance at which the linearly propagating beam doubles its initial width). Hence, the linear and nonlinear propagation can be hardly distinguished experimentally.

One way to overcome the problem of the short mode propagation length is to introduce gain into the dielectric medium, by using, for example, a quantum well or quantum dot system [29]. From Eq. (4), we find that the required gain coefficients are $\gamma_0 = 400\ \mathrm{cm}^{-1}$ and $\gamma_{\pi/D} = 2700\ \mathrm{cm}^{-1}$. Those levels of gain, while within the theoretically possible limits, are extremely high, hence, rendering the underlying configuration somewhat impractical.

To provide a feasible way for experimental observation of subwavelength solitons we set the working wavelength to 1.55 μm, and fix the widths of the silver and the dielectric slabs at 28 and 60 nm, respectively. Changing the working wavelength results in a decrease of the power transferred through the metal, due to the increasing ratio between the real parts of the dielectric constants ($\varepsilon_m = -130 + 3.68i$) [25]. Consequently, the modes' propagation loss is substantially decreased. Moreover, the decreased field penetration to the metal, together with the increased metal slab width, results in a significantly weaker coupling (tunneling) between neighboring slabs. As a result, the propagation band flattens and becomes more symmetric compared to that in the visible range.

The electric field components of the localized modes with a moderate index change of 0.02 are given in Fig. 3(a) for the $k_x = 0$ mode and in Fig. 3(c) for $k_x = \pi/D$, respectively. The corresponding intensities are presented in Figs. 3(b) and 3(d). In contrast to the previous case, here both modes exhibit subwavelength widths of 420 nm. Furthermore, since the modal effective index is $n_{\mathrm{eff}} = \beta/k_0 \approx 1.78$, the mode size is lower than the diffraction limit in the MDMLs ($1.22\lambda_0/2n_{\mathrm{eff}} = 530$ nm), and can be reduced to $\sim$200 nm if nonlinear index change of 0.1 is used [26]. Hence, we choose to focus on the mode at $k_x = 0$, whose propagation loss $\alpha_0 = 123\ \mathrm{cm}^{-1}$ (decay length of 80 μm) is much smaller than the $k_x = \pi/D$ mode with $\alpha_{\pi/D} = 1280\ \mathrm{cm}^{-1}$ (decay length of 7.8 μm).

Figures 3(e) and 3(f) compare the linear and nonlinear propagation of the mode at $k_x = 0$ in lossless MDMLs, showing stationary propagation over more than two diffraction lengths when nonlinearity is applied. To realize a practical experiment, we have simulated the linear and nonlinear propagation of a simple Gaussian beam at a width of 380 nm in MDMLs with the metal loss taken into account [Figs. 3(g) and 3(h), respectively]. While the linearly propagating beam doubles its width after 20 μm, the nonlinearly propagating wave packet maintains its original shape (with somewhat attenuated intensity). Thus, an experimental observation of subwavelength discrete solitons can be realized even without a gain medium. On the other hand, perfect solitary propagation requires a moderate gain of $\gamma_0 = 100\ \mathrm{cm}^{-1}$.

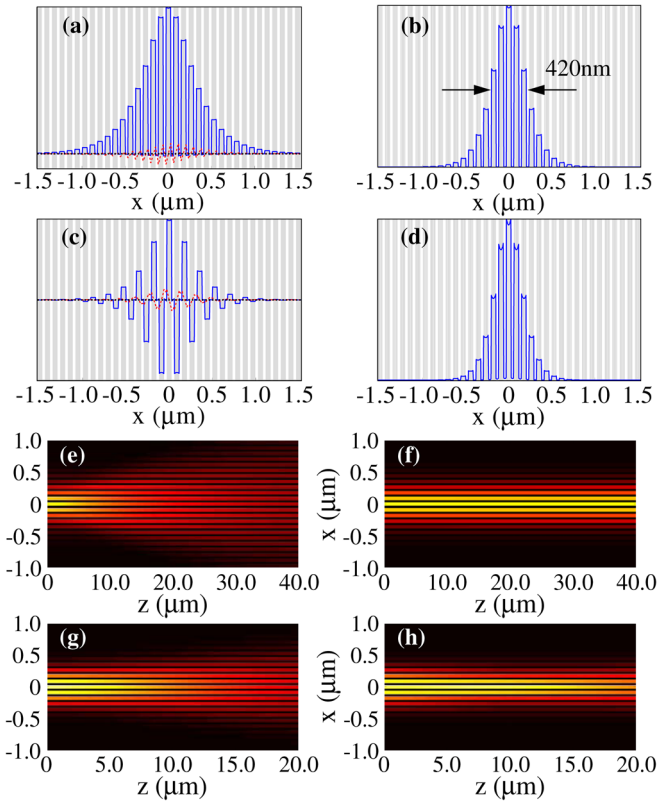

FIG. 3 (color online). Nonlinear localized EM modes in MDMLs with period of 88 nm at an incident wavelength of 1.55 μm. (a)–(d) are the same as Figs. 2(c) and 2(d). (e) Linear and (f) nonlinear propagation of the $k_x = 0$ mode over 40 μm distance in lossless MDMLs. (g) Linear and (h) nonlinear propagation of a wave packet excited by a Gaussian beam along 20 μm in a MDML when the silver's loss is taken into account.

A recent study has shown formation of spatial solitons in a Kerr medium embedded between two semi-infinite metals [30]. Such solitons originate from the balance between diffraction in the homogeneous medium and the Kerr nonlinearity, and are inherently different than the solitons arising from the nonlinear counteraction of the SPPs tunneling, presented in this Letter. Moreover, the subwavelength mode size, claimed in [30], is not due to the nonlinear diffraction arrest; it arises from the SPP *linear* confinement in the direction normal to the plane of propagation. In this Letter, we present the first subwavelength SPP soliton with the mode size determined entirely by the interplay between SPPs tunneling and Kerr nonlinearity.

To summarize, we have theoretically shown subwavelength discrete solitons in nonlinear MDMLs. The formation of such solitons is a result of the threefold interplay between periodicity, nonlinearity, and surface plasmons tunneling, leading to new and intriguing phenomena that are not found in nonlinear DWGAs. We have addressed the issue of the intrinsic loss in such structures, calculated the gain required to compensate such losses, and suggested a feasible configuration in which subwavelength discrete solitons could be experimentally observed. We expect that these exciting findings will inspire both experimental and theoretical efforts towards studies of a wide range of nonlinear metamaterials, for applications in the emerging field of subwavelength nonlinear optics.

The authors are grateful to Ofer Manela, Dr. Oren Cohen, and Professor Yuen-Ron Shen for valuable discussions. This work was supported by AFOSR MURI program (FA9550-04-1-0434) and NSF NSEC (DMI0327077).

*xiang@berkeley.edu

[1] V. G. Veselago, Sov. Phys. Usp. **10**, 509 (1968).
[2] R. A. Shelby, D. R. Smith, and S. Schultz, Science **292**, 77 (2001).
[3] J. B. Pendry, D. Schurig, and D. R. Smith, Science **312**, 1780 (2006).
[4] M. W. Klein *et al.*, Science **313**, 502 (2006).
[5] N. Lazarides, M. Eleftheriou, and G. P. Tsironis, Phys. Rev. Lett. **97**, 157406 (2006).
[6] A. A. Zharov, I. V. Shadrivov, and Y. S. Kivshar, Phys. Rev. Lett. **91**, 037401 (2003).
[7] H. Raether, *Surface Plasmons: On Smooth and Rough Surfaces and on Gratings* (Springer, Berlin, 1988).
[8] T. W. Ebbesen *et al.*, Nature (London) **391**, 667 (1998).
[9] N. Fang *et al.*, Science **308**, 534 (2005).
[10] E. N. Economou, Phys. Rev. **182**, 539 (1969).
[11] J. Schilling, Phys. Rev. E **74**, 046618 (2006).
[12] R. S. Bennink *et al.*, Opt. Lett. **24**, 1416 (1999).
[13] M. Scalora *et al.*, Phys. Rev. E **73**, 016603 (2006).
[14] A. S. Davydov, J. Theor. Biol. **38**, 559 (1973).
[15] W. P. Su, J. R. Schrieffer, and A. J. Heeger, Phys. Rev. Lett. **42**, 1698 (1979).
[16] A. Trombettoni and A. Smerzi, Phys. Rev. Lett. **86**, 2353 (2001).
[17] D. N. Christodoulides and R. I. Joseph, Opt. Lett. **13**, 794 (1988).
[18] H. Eisenberg *et al.*, Phys. Rev. Lett. **81**, 3383 (1998).
[19] D. N. Christodoulides *et al.*, Nature (London) **424**, 817 (2003).
[20] Y. S. Kivshar, Opt. Lett. **18**, 1147 (1993).
[21] J. W. Fleischer *et al.*, Phys. Rev. Lett. **90**, 023902 (2003).
[22] D. Mandelik *et al.*, Phys. Rev. Lett. **90**, 053902 (2003).
[23] O. Cohen *et al.*, Phys. Rev. Lett. **91**, 113901 (2003).
[24] R. Morandotti *et al.*, Phys. Rev. Lett. **86**, 3296 (2001); T. Pertsch *et al.*, Phys. Rev. Lett. **88**, 093901 (2002).
[25] P. B. Johnson and R. W. Christy, Phys. Rev. B **6**, 4370 (1972).
[26] An index change at the order of 0.1 was reported [e.g., L. Brzozowski *et al.*, Appl. Phys. Lett. **82**, 4429 (2003)].
[27] M. D. Feit and J. A. Fleck, Appl. Opt. **17**, 3990 (1978)
[28] We modify the linear part of the standard BPM by projecting the initial wave packet on the linear MDML's modes [calculated according to Eq. (4)], instead of using the plane wave expansion (i.e., Fourier transform). This modification allows for modeling the propagation of wave functions with subwavelength feature size, which is essential for studying SPPs propagation.
[29] R. D. Schaller *et al.*, J. Phys. Chem. B **107**, 13 765 (2003).
[30] E. Feigenbaum and M. Orenstein, Opt. Lett. **32**, 674 (2007).